Dynamics of geminate charge separation in liquid methylcyclohexane studied by the photoassisted ion pair separation technique

ARTICLE *in* CHEMICAL PHYSICS · NOVEMBER 1996

Impact Factor: 1.65 · DOI: 10.1016/0301-0104(96)00149-8

4 AUTHORS, INCLUDING:

Victor A Nadtochenko
Russian Academy of Sciences
110 PUBLICATIONS **1,549** CITATIONS
SEE PROFILE

Leonid Victorovich Lukin
Russian Academy of Sciences
32 PUBLICATIONS **118** CITATIONS
SEE PROFILE

ELSEVIER

Chemical Physics 211 (1996) 469–488

Chemical Physics

Dynamics of geminate charge separation in liquid methylcyclohexane studied by the photoassisted ion pair separation technique

F.F. Brazgun [a], V.A. Nadtochenko [a], I.V. Rubtsov [a], L.V. Lukin [b,*]

[a] *Institute of Chemical Physics in Chernogolovka, Russian Academy of Sciences, Chernogolovka, 142432 Moscow Region, Russian Federation*

[b] *Institute for Energy Problems of Chemical Physics, Russian Academy of Sciences, Chernogolovka, 142432 Moscow Region, Russian Federation*

Received 14 December 1995; in final form 13 May 1996

Abstract

A laser photoassisted ion pair separation technique has been developed to study the kinetics of geminate charge recombination in the picosecond domain in hydrocarbon liquids. Recombination of geminate pairs in liquid methylcyclohexane has been studied by this technique. The electrons were created by two-photon ionization of the anthracene and tetramethyl-p-phenylenediamine (TMPD) admixture using a picosecond UV laser pulse at 270 or 360 nm and then were excited by an IR laser pulse at 1080 nm. The diffusion model of photostimulated ion pair dissociation has been extended to the picosecond time regime in order to describe the observed dependence of the IR enhanced photoconductivity of the solutions on the time delay between the UV and IR pulses. The average initial separation between a geminate trapped electron and its sibling cation was obtained from the experimental decay curves of the IR enhanced photocharge. The separation in the geminate electron–cation pair was found to increase with initial excess excitation energy, ΔE, of the solute above its ionization threshold. It is concluded that the hot electron, the precursor of the trapped geminate electron, is initially injected into the liquid with kinetic energy that increases with increasing the ΔE energy.

1. Introduction

Generation of charge carriers on the photoexcitation of molecular media above the ionization threshold involves a succession of fast electron processes: autoionization of excited states followed by injection of electrons into the medium, electron thermalization, localization in traps and solvation due to reorganization of solvent [1–4]. As a result, a geminate ion pair consisting of the trapped (solvated) electron e_t^- and its sibling cation A^+, bound together by the Coulomb attraction, is produced after photoionization.

A knowledge of the initial spatial distribution of the geminate pair (e_t^-, A^+) is of great importance both for the elucidation of the mechanism of ionization and for a study of all further reactions of e_t^-. In fact, the distribution of e_t^- with respect to its parent cation depends not only on the energy of highly excited states A^*, precursors of electrons injected, but also on the electron–solvent interaction that de-

* Corresponding author. Fax: +7 095 137 34 79.

PII S0301-0104(96)00149-8

termines the distance the electron travels in the medium till the formation of equilibrated states e_t^- occurs [4–6]. One of the direct ways of studying the electron–cation spatial distribution in molecular liquids is to follow the recombination kinetics of the pair (e_t^-, A^+) [4]. The smaller the initial distance between e_t^- and A^+, the greater the rate of their geminate recombination. The introduction of femtosecond pulse UV lasers as a photoionization source has made it possible to study the geminate recombination in the subpicosecond domain both in polar [7–11] and nonpolar [7,12,13] liquids. Contrary to the electron pulse radiolysis, the principal method employed in these studies last 30 years, the two-photon UV laser ionization allows for preparation of a well-defined narrow distribution in energy of initial excitations and electrons initially injected into liquid.

Last 15 years, a kinetic laser technique, called the photoassisted ion pair separation (PAIPS) technique, was developed to study the geminate recombination in nonpolar matrices [14]. It is based on the phenomenon of the enhancement of free ion yield (i.e. the yield of electron–ion pairs that do not undergo geminate recombination) in a photon absorption by a geminate electron. The effect of an electron photoexcitation on the probability of the geminate pair dissociation has been observed at first in 3-methylpentane glass [15] and, lately, in hydrocarbon liquids [16–26]. The increase of the pair dissociation probability has been attributed [14–18] to the formation in the process

$$e_t^- + h\nu \rightarrow e_{hot}^- \rightarrow e_t^- \qquad (1.1)$$

of the quasi-free "hot" electron e_{hot}^- which conserves for a some time its excess kinetic energy above thermal one. In the kinetic PAIPS method [16,18,22,25], the ion pairs (e_t^-, A^+) are produced by photoionization of solute molecules, A, with the UV laser pulse followed by excitation of the geminate electrons by the second pulse of the IR or visible region. An increase, ΔQ, of the photogenerated charge due to additional action of the second pulse is measured as a function of a delay time, t_d, between pulses. In Refs. [18,20], a simple diffusion model of photostimulated charges separation has been suggested. This model predicts that at short t_d the dependence of ΔQ on t_d carries the information on the initial spatial distribution of the pair (e_t^-, A^+). Since the life times of electron–ion pairs in liquids lie usually in the subnanosecond range, it is interesting to determine the dependence $\Delta Q(t_d)$ in the picosecond domain and find from it the initial pair separation. Although the picosecond decay kinetics of the PAIPS signal was investigated [22,23,25,26], the comparison between experiment and the model suggested in Refs. [18–20] has not been made yet in detail.

The goal of the work reported here is to continue in studies on optically stimulated charge pair dissociation in the picosecond domain and obtain, using the PAIPS method, new experimental data on the recombination rate of the geminate pairs formed in solutions of anthracene and tetramethyl-p-phenylenediamine (TMPD) in methylcyclohexane. In addition, we try to determine the initial distance distribution within the geminate pair by comparing the observed decay $\Delta Q(t_d)$ with the decay curves calculated within the diffusion model. By choosing the solutes with different ionization potentials, we have a chance of covering the interval of 3 eV in the initial excitation energy above the ionization threshold of a solute at used wavelengths of the UV laser radiation $\lambda_{UV} = 270$ nm and $\lambda_{UV} = 360$ nm.

It is shown below that for two-photon ionization of the aromatic solute A (anthracene or TMPD) the initial distance between e_t^- and A^+ increases with increasing the initial excitation energy of the solute above its ionization threshold. Our results agree with a simple photoionization picture in which the hot electron e_{hot}^-, the immediate precursor of e_t^-, is assumed to be initially created in the process

$$A + 2h\nu_{UV} \rightarrow A^* \rightarrow e_{hot}^- \rightarrow \text{thermalization} \rightarrow (e_t^-, A^+). \qquad (1.2)$$

The observed increase of distance between e_t^- and A^+ seems to be due to the increase of the initial kinetic energy of e_{hot}^- with increasing excitation energy of A^* (here $h\nu_{UV}$ is the photon energy of the UV light).

2. Experimental procedure

Methylcyclohexane (MCH) was degassed with freeze–pump–thaw cycles and purified from electron

acceptors by metallic Na and by molecular sieves. The life times of excess electrons in the purified solvent was about 10^{-5} s. Experiments were done on solutions of anthracene in MCH at the solute concentration of 2×10^{-5} M, and solutions of TMPD in MCH at 2×10^{-4} M.

We used two photoconductivity quartz cells containing two parallel stainless steel plate electrodes with area about 0.4×0.6 cm^2. The distance between electrodes was about $d = 0.32$–0.34 cm in one cell and about $d = 0.35$ cm in the other.

The electrons were created by the two-photon ionization of solutions with the UV laser pulses from the third ($\lambda_{UV} = 360$ nm) or forth ($\lambda_{UV} = 270$ nm) harmonics of hybrid active–passive mode locked Nd^{3+} aluminate laser. Thereupon the electrons were excited by the IR pulses of the first harmonic ($\lambda_{IR} = 1080$ nm). The light pulse duration was about 19 ps. The spectral conversion of the 1080 nm light to the second, third and fourth harmonics was carried out by the KDP crystals. The laser pulse energy was measured by photodiodes and recorded by the computer.

The UV laser pulses illuminated the liquid between electrodes along greater side of the electrodes. The optical path length, l_{opt}, was about $l_{opt} = 0.6$ cm. Following the arrival of the UV pulse, the IR pulse at 1080 nm delayed for a time, t_d, has illuminated the same ionized part of the solution. The angle between the directions of the UV and IR laser beams was about 2°. In order to keep out the laser light from action on the electrodes, the cross-sectional area of the laser beam was bounded with a diaphragm of the area, s, about $s = a^2 \approx 0.3 \times 0.3$ cm^2. Thus, the volume of the sample ionized by the laser was about $\Delta v = l_{opt} s \approx 0.05$ cm^3. The energy, Φ_{IR}, of the IR light was not more than 3–4 mJ a pulse.

The electric scheme of the photoconductivity measurements was similar to that described in Refs. [16,17]. A potential difference, V, of 2 kV was maintained across the electrodes. At such V the photocurrent transient lasted for about 0.05 s until ions arrived at electrodes. Transient photocurrent signals were measured across a load resistor of 2×10^9 Ω. In this case, the characteristic response time of a current circuit was about 0.3 s. Thus, we have measured the total integral over time of a free ion photocurrent induced by the picosecond laser pulses, i.e. the total electric charge collected on the electrodes.

3. Experimental results

The dependence of the free ion electric charge, Q, photogenerated in the solutions by the UV laser pulse, acting alone, on the UV light intensity, u_{UV}, was quadratic in u_{UV} at low u_{UV} and became superlinear (between linear and quadratic) at high u_{UV}. Because of this a gate around a fixed value of u_{UV} was established so that the pulses falling out of the gate were rejected. In addition, the UV light intensity was restricted to the condition for a small bulk decay of photogenerated charge carriers caused by their bulk recombination. So the UV light intensity and, hence, the average concentration of ions, n_{ion}, was reduced until the condition

$$t_{fl}/t_{rec} \ll 1 \tag{3.1}$$

was fulfilled. Here $t_{fl} = ad/\mu_{ion}V$ denotes the time of ion flight through the size, a, of a laser spot, $t_{rec} = (k_{rec} n_{ion})^{-1}$ is the time of the bulk recombination, μ_{ion} is the sum of mobilities of positive and negative ions, k_{rec} is the recombination rate constant. When (3.1) holds the measured charge Q is proportional to the probability, q, for an electron–cation pair to escape geminate recombination, i.e.

$$Q \approx eNq, \tag{3.2}$$

where e is the electron charge, N is the initial number of geminate pairs produced by the UV pulse in liquid between electrodes. A criterion for the condition (3.1) was a small increase of Q (by 20–30% at room temperature) with increasing V from 1 up to 2 kV. This agrees with the external electric field dependence of q in the Onsager model [27] in which the dissociation probability of a geminate pair equals $q = q_0(1 + eHr_c/2k_BT)$ for low electric fields H where q_0 is the zero field dissociation probability, $H = V/d$ is an external electric field applied, k_B is the Boltzmann constant, T is the temperature, $r_c = e^2/\varepsilon k_B T$ is the Onsager radius, $\varepsilon = 2.02$ is dielectric constant. Another criterion for the fulfillment of (3.1) was a small measured charge $Q < 0.5 \times 10^{-11}$ C in comparison with the effective electric charge at

the electrodes of the cell $Q_c = C_{cel}V \approx 2 \times 10^{-10}$ C at $V = 2$ kV where $C_{cel} = \varepsilon a l_{opt}/4\pi d \approx 1 \times 10^{-13}$ F is the effective capacity of the cell. Really, it can be shown that (3.1) corresponds to the relationship $Q/Q_c \ll 1$ (we assumed here that $Q \approx en_{ion}a^2 l_{opt}$ and $k_{rec} = 4\pi\mu_{ion}e/\varepsilon$ in nonpolar liquids).

The photocurrents induced by the UV pulses in the pure solvent were much below the signals observed in the solutions of anthracene and TMPD. No photocurrent was observed when only the IR pulse illuminated the solutions. The cooperative action of both a UV and an IR pulse, separated in time, generated a larger photocurrent than the UV pulse acting alone. The enhancement, ΔQ, of free ion charge decreased with increasing time delay, t_d, between the UV and IR pulses. Here $\Delta Q = Q_{sum} - Q$ where Q and Q_{sum} are free ion charges photogenerated only by the UV pulse and by the cooperative action of the UV and IR pulses, respectively. However, the dependence of ΔQ on t_d in the solution of TMPD was distinct from that in the anthracene solution.

3.1. Decay kinetics of the IR enhanced photocurrent in solutions of anthracene

Fig. 1 shows the dependence of $\Delta Q/Q$ on t_d observed in solutions of anthracene at two wavelengths of the UV laser radiation: 360 and 270 nm. The decay kinetics $\Delta Q(t_d)$ was investigated in the temperature interval 220–293 K.

As a whole, the observed dependencies of ΔQ on t_d exhibit all the peculiarities revealed previously for solutions of anthracene in n-hexane, MCH and squalane at nanosecond [16–18,20] and picosecond [22–26] time delays. As seen from Fig. 1a and Fig. 1b, the decay time at half-maximum increases with decreasing temperature. At all temperatures studied, the decay time for $\lambda_{UV} = 270$ nm was greater than that for $\lambda_{UV} = 360$ nm. Absolute values of $\Delta Q/Q$ increased with cooling of the liquid and with increase of the UV wavelength. For example, as seen from Fig. 1, at $\lambda_{UV} = 360$ nm and $\Phi_{IR} = 3$ mJ the values of $\Delta Q/Q$ measured at a small delay $t_d \approx 30$ ps are about 3 and 8.5 at temperatures 293 and 220 K, respectively. The dependence of ΔQ on the 1080 nm light intensity was close to linear.

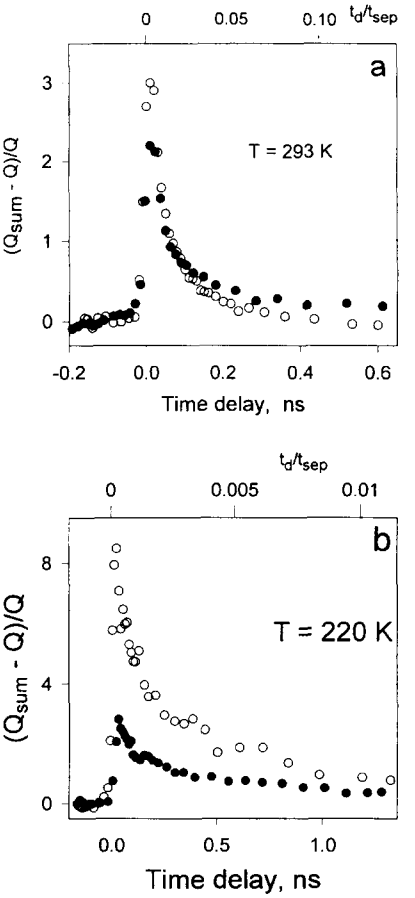

Fig. 1. The relative enhancement of the infrared-induced photocurrent as a function of time delay between UV and IR pulses for the solution of anthracene in methylcyclohexane at $T = 293$ K (a) and 220 K (b). Open points correspond to $\lambda_{UV} = 360$ nm, filled points to $\lambda_{UV} = 270$ nm, $\Phi_{IR} = 3$ mJ. The upper scale shows the dimensionless time delays at $t_{sep} = 4.5$ ns (a) and $t_{sep} = 118$ ns (b).

3.2. Decay kinetics of the IR enhanced photocurrent in the TMPD solutions

Contrary to the solutions of anthracene, the dependence of ΔQ on t_d observed in the solutions of TMPD has two components: a fast decay with a half-life of the order of 50 ps at room temperature and then a weakly falling plateau that does not practically decay during, at least, 1 ns. Fig. 2 demonstrates the IR enhanced photocharge ΔQ versus time delay obtained at $\lambda_{UV} = 360$ nm and two different energies of the IR pulse. Each decay curve in Fig. 2

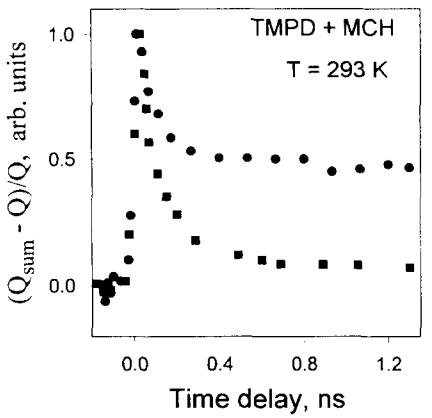

Fig. 2. The enhancement of the IR induced photocharge as a function of time delay in the solution of TMPD at 293 K. The wavelength of the UV laser was $\lambda_{UV} = 360$ nm. Circular points correspond to $\Phi_{IR} = 1.3$ mJ, square points to $\Phi_{IR} = 0.2$ mJ. Each experimental curve has been normalized to unit at its maximum.

is scaled to unity at its maximum. As seen, the decay kinetics $\Delta Q(t_d)$ depends on the energy, Φ_{IR}, of the IR pulse. At $T = 293$ K and short time delays (~ 20 ps) the dependence of ΔQ on Φ_{IR} was linear while at large $t_d > 400$ ps the value of ΔQ was quadratic in Φ_{IR}.

The slow component of the decay curve $\Delta Q(t_d)$, which did not drop at $t_d = 1$ ns, was attributed to two-photon ionization by the IR pulse of the first-excited singlet states S_1 of TMPD:

$$S_1 + 2h\nu_{IR} \rightarrow e_t^- + TMPD^+. \qquad (3.3)$$

Such an assumption agrees with the long life time (4.3 ns [28,29]) of the TMPD singlets and does not contradict the threshold energy 1.68 ± 0.06 eV for one photon ionization of the first-excited singlet state of TMPD in n-hexane [30].

In order to lower the contribution of the process (3.3) into the ΔQ signal, we reduced the energy of the IR pulse down to values of $\Phi_{IR} \approx 0.15$–0.3 mJ until the enhancement, ΔQ, of charge at $t_d = 1$ ns became not more than 10% from the maximum value of ΔQ measured at short time delays. (At such small Φ_{IR} the maximum value of $\Delta Q/Q$ in the peak of the $\Delta Q(t_d)$ curve was about 0.3–0.5.) Then, using a magnitude of ΔQ at $t_d = 1$ ns and known life time (4.3 ns) of S_1, we subtracted the contribution of the slow component from the experimental curve $\Delta Q(t_d)$. As can be seen from Fig. 2 and Fig. 3, the first decay time at half-maximum of the prompt component of the IR enhanced photocurrent increases with cooling from about 50 ps at $T = 293$ K up to about 400 ps at $T = 248$ K.

Both the increase of free ion charge ΔQ in the solutions of anthracene and the prompt component of the decay curve $\Delta Q(t_d)$ in the solutions of TMPD in methylcyclohexane were attributed to the excitation of geminate electrons e_t^- by the IR pulse resulting in formation of the hot electrons e_{hot}^-. It has been noted [16–20,23] that at a large enough distance between e_t^- and A^+ the hot electron, created in the process (1.1) after the IR photon absorption, does not recombine before thermalization, but forms after thermalization and localization a new pair $(e_t^-, A^+)^N$, see scheme (3.4). Because of high effective temperature of e_{hot}^-, the mean dissociation probability, q_1, of the new pair $(e_t^-, A^+)^N$ is thought [17–19] to be greater than that of the pair (e_t, A^+). If the condition (3.1) holds then $\Delta Q/Q = \Delta q/q$ where $\Delta q = q_1 - q$ is the IR pulse enhanced dissociation probability of the pair.

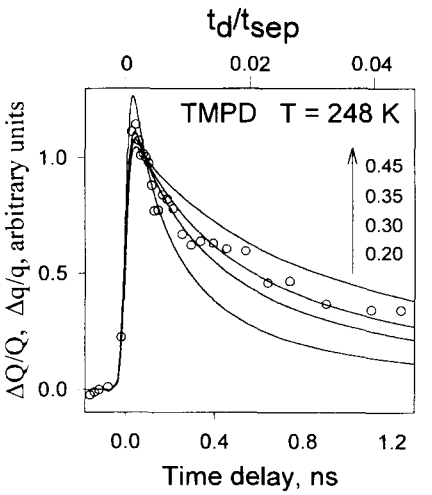

Fig. 3. Comparison between the experimental decay kinetics $\Delta Q(t_d)$ observed in the solution of TMPD at $T = 248$ K, $\lambda_{UV} = 270$ nm (points) and the time dependences $\Delta q(t_d)$ calculated from Eq. (4.17). Each curve has been scaled to unit at $t_d = t^* = 88.5$ ps. The numbers near the vertical arrow are the parameters $b = B/r_c$ of the initial function $f_0(r)$ corresponding to the calculated curves. The upper scale shows $\tau_d = t_d/t_{sep}$. The used parameters are: $\varepsilon = 2.091$, $r_c = 32.2$ nm, $D = 3.68 \times 10^{-4}$ cm^2 s^{-1} and $t_{sep} = 28$ ns.

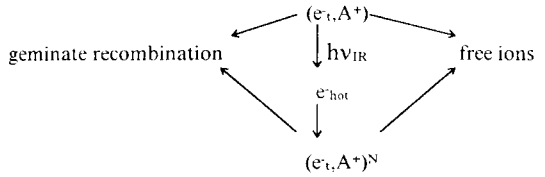

(3.4)

The scheme (3.4) allows an understanding of the observed dependencies of the decay curves $\Delta Q(t_d)$ on temperature and on the UV laser wavelength. Really, the lower the temperature, the smaller the mobility of e_t^- and hence the greater the number of geminate electrons surviving by the time $t = t_d$. On the other hand, the less the wavelength λ_{UV}, the greater the initial distance between e_t^- and A^+ and hence the greater the characteristic decay time of the survival probability of the geminate pair (e_t^-, A^+). Such arguments have allowed to explain qualitatively within the scheme (3.4) experimental data on the IR enhanced photocurrent observed previously in solutions of anthracene at the nanosecond [16–18] and picosecond [22–26] time delays.

To make a rough estimate of Δq, let us first consider the photon absorption of electrons trapped at a fixed distance, r, from their parent cations A^+. According to Onsager's theory [27], in the darkness the probability for such electrons to escape geminate recombination is $q = \exp(-r_c/r)$. In the case of infinitely high temperature of photoliberated electron e_{hot}^-, its motion is not significantly perturbed by the Coulomb field of the cation. The most simple estimation of Δq can be obtained under the assumption that after thermalization a half of hot electrons is solvated at distance $r + L$ from A^+ and a half at distance $r - L$ where L is a mean solvation length of e_{hot}^-. In this case, a mean dissociation probability of the new pairs formed after the single concurrent photoexcitation of all electrons is

$$q_1 = \{\exp[-r_c/(r+L)] + \exp[-r_c/(r-L)]\}/2. \tag{3.5}$$

From this follows that, for example, at $r_c = 50$ nm, $r = 6$ nm and $L = 3$ nm the relative increase of escape probability per one IR photon absorbed is $\Delta q/q = (q_1 - q)/q \approx 6.4$. This agrees with large values of $\Delta Q/Q \approx 10$–100 observed at low temperatures in solutions of anthracene in n-hexane [16] and methylcyclohexane [17] when a lot of IR photons were repeatedly absorbed by a geminate electron during the nanosecond IR pulse. On the other hand, at $r \gg L$ and $Lr_c/r^2 \ll 1$ we obtain

$$\frac{\Delta q}{q} = \frac{(q_1 - q)}{q} \approx \frac{Lr_c}{r^2}. \tag{3.6}$$

As seen, $\Delta q/q \to 0$ at $r \to \infty$ when the photoexcitation of free electrons occurs. Thus, the contribution from the photoexcited electron e_t^- into the PAIPS signal depends on r and L. Such simple considerations demonstrate the distinction between the kinetic PAIPS technique and a commonly used pump-and-probe one. In the latter case, the contribution of e_t^- into the optical absorption signal induced by the pump pulse does not depend on the distance between electron and its parent cation and the time dependent electron absorption, contrary to the PAIPS signal, is proportional to the survival probability of the geminate pairs.

Below we report a calculation of Δq within a simple diffusion model [18,19,21] which allows one to find the initial distribution function $f_0(r)$ of the distances, r, between geminate charges e_t^- and A^+ from the experimental decay kinetics $\Delta Q(t_d)$.

4. Diffusion model of the optically stimulated geminate pair dissociation

To establish a link between Δq and $f_0(r)$, we shall follow the approach of Refs. [18,19,21] and use the following further assumptions.

1. The full thermalization and solvation time, t_0, of the hot electron in liquid MCH is much less than the laser pulse duration $t_p = 20$ ps. Moreover, the t_0 time is assumed to be less than the average time interval between two successive events of an IR photon absorption by an electron, i.e. $t_0 < (\sigma u)^{-1}$ where σ is the photoionization cross section of trapped electrons at 1080 nm, $u = \Phi_{IR}/h\nu_{IR}t_p s$ is the IR laser intensity (in cm^{-2} s^{-1}), $s \approx 0.09$ cm^2 is the cross sectional area of the laser beam, $h\nu_{IR} = 1.15$ eV is the IR photon energy. Assuming that σ equals the electron absorption cross section 3×10^{-17} cm^2 at 1080

nm [31], the latter supposition seems to be justified at $t_0 < 1$ ps and, at least, at energies $\Phi_{IR} < 2$ mJ when $u\sigma < 2.5 \times 10^{11}$ s^{-1} and therefore $u\sigma t_0 < 0.25$.

2. At $t > t_0$ after the injection of electron into the liquid the motion of e_t^- can be described by the time independent diffusion coefficient D.
3. In darkness the probability density $f(t,r)$ for the trapped electron to be in the elemental volume d^3r at the distance r from its parent cation satisfies the Smoluchowski equation

$$\frac{\partial}{\partial t} f = D\left[\frac{\partial^2 f}{\partial r^2} + \left(\frac{2}{r} + \frac{r_c}{r^2}\right)\frac{\partial f}{\partial r}\right], \qquad (4.1)$$

with the initial condition $f = f_0(r)$ at $t = 0$. The distribution function $f_0(r)$ is normalized by the condition $\int f_0 \, d^3r = 1$.

First we consider that the geminate pairs (e_t^-, A^+) are created at $t = 0$. In the absence of external electric field and electron photoexcitation the separation probability of the pair is

$$q_0 = \int f_0(r) P(r) \, d^3r = \int f(t,r) P(r) \, d^3r, \qquad (4.2)$$

where $P = \exp(-r_c/r)$ is the escape probability of a single charge pair with the distance r between partners [27]. As well as in the works [19–21], we shall describe the photostimulated electron transfer rate in the process (1.1) by two parameters: the mean squared solvation distance of a photoliberated electron in the absence of electric field

$$L = \left(4\pi \int_0^\infty \rho^4 b(\rho) \, d\rho\right)^{1/2} \qquad (4.3)$$

and its drift displacement, Δ_e, in an unit electric field, see Fig. 4. Both L and Δ_e describe the electron motion for a full thermalization and solvation time t_0 since the inception of e_{hot}^- after an IR photon absorption by e_t^- until the formation of a new equilibrated trapped state e_t^- in the process (1.1). (The function $b(\rho)$ is the probability density for the e_{hot}^- electron to be trapped at distance ρ from the initial position of e_t^- by the time of its photoionization. It is normalized by the condition: $4\pi \int_0^\infty \rho^2 b \, d\rho = 1$.) The value of Δ_e/t_0 means an average mobility of a photoliberated electron. For the hot electron in methylcyclohexane these parameters have been measured previously. The length $L = 6 \pm 1$ nm was obtained from

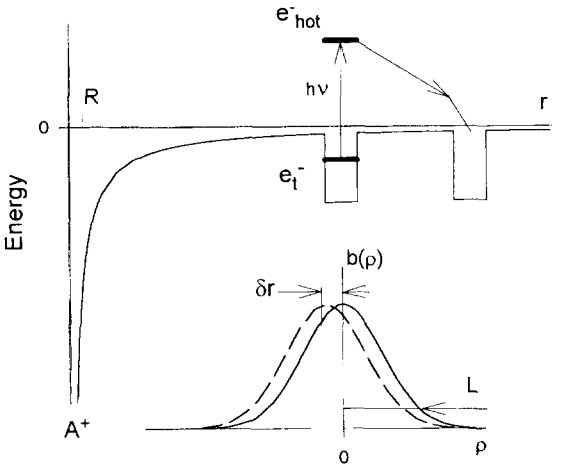

Fig. 4. The mechanism of photoassisted electron migration from one trap to another discussed in the text. The solid curve in the bottom of the picture shows the spatial distribution $b(\rho)$ of trapped electrons just after thermalization and solvation of e_{hot}^- in the absence of the Coulomb field. The dashed line shows that the distribution becomes displaced a distance δr in the direction of the Coulombic centre where $\delta r = \Delta_e H_c$ and $H_c = e/\varepsilon r^2$.

the PAIPS experiments in the nanosecond domain [19,21] and the drift displacement Δ_e was found from the measurements of the photocurrent transients arising from the photoexcitation of free electrons: $(5 \pm 1) \times 10^{-13}$ cm^2 V^{-1} at $T = 150$–210 K from Ref. [32] and $(7 \pm 1.5) \times 10^{-13}$ cm^2 V^{-1} at 150–190 from Ref. [21]. It is worth noting that the measurements of Δ_e were performed in the conditions when the excitation of e_t^- by the nanosecond IR laser pulse occurred far away from the Coulombic centre.

We also ignore the effect of the IR laser field on the relaxation rate of e_{hot}^-, because at the used light intensity the rate of the photostimulated transfer $e_{hot}^- \rightarrow e_t^-$ is expected to be much less than the electron relaxation rate due to elastic and inelastic electron scattering: $u\sigma \ll v/\lambda_{inl} = 5 \times 10^{13}$–$3 \times 10^{14}$ s^{-1} and $u\sigma \ll v/\lambda_{el} \approx (0.5$–$1) \times 10^{15}$ s^{-1} where $v \approx 5 \times 10^7$ cm/s is the velocity of the hot electron corresponding to its initial energy of 0.8 eV (see Section 6), $\lambda_{inl} = 2$–10 nm and $\lambda_{el} = 0.5$–1 nm are the electron mean free paths before inelastic and elastic scattering, respectively, in hydrocarbon matrices [5,33,34].

Following Ref. [19], let us find, at first, the enhancement of the dissociation probability caused

by the photoexcitation of electrons by an infinitely short IR pulse in the limit of small displacements of e^-_{hot}:

$$\Delta_e H_c \ll r,\ L \ll r, \tag{4.4}$$

where $H_c = e/\varepsilon r^2$ is the Coulombic field. Calculations made below show that at $\Delta_e = 6\times 10^{-13}$ cm^2/V and $L \approx 5$ nm this condition is valid for most geminate pairs at $t_d > 0.003 r_c^2/D$.

When (4.4) holds, a single photoexcitation of all electrons at $t = t_d$ results after solvation of e_{hot} in a new distribution $f_1^N(t_d,r)$ that differs little from $f(t_d,r)$. The change in distribution $\delta f_1 = f_1^N(t_d,r) - f(t_d,r)$, as shown in Refs. [19,21], can be presented as

$$\delta f_1 = \frac{L^2}{6}\left[\frac{\partial^2}{\partial r^2} + \left(\frac{2}{r} + \frac{e^2}{\varepsilon k_B T_{ef} r^2}\right)\frac{\partial}{\partial r}\right] f(t_d,r), \tag{4.5}$$

where the parameter T_{ef}, called the effective temperature of photoliberated electron e^-_{hot}, is defined as

$$T_{ef} = \frac{eL^2}{6k_B\Delta_e}. \tag{4.6}$$

As one might expect, at $t_0 \to 0$ the relationship (4.5) corresponds to the Smoluchowski equation for the charge particle with temperature T_{ef} and diffusion coefficient $L^2/6t_0$. (For a thermalized charge particle with diffusion coefficient D_0 and mobility m_0 the effective temperature equals $T_{ef} = T$ because, in this case, $L^2 = 6D_0 t_0$, $\Delta_e = m_0 t_0$ and the values of D_0 and m_0 are related by the Nernst–Einstein relationship $D_0 = m_0 k_B T/e$.) The enhancement, Δq_1, of the escape probability due to a single photoexcitation of all trapped electrons at $t = t_d$ becomes

$$\Delta q_1 = \int \delta f_1 P\, d^3r = \frac{L^2}{6r_c^2}\left(1 - \frac{T}{T_{ef}}\right) z(t_d), \tag{4.7}$$

$$z = 4\pi\int_R^\infty r^{-2} r_c^4 f(t_d,r) P\, dr$$

$$= 4\pi\int_{R/r_c}^\infty x^{-2} F(\tau_d,x)\exp(-1/x)\, dx, \tag{4.8}$$

where R is the recombination radius of e_t^- (of the order of molecular size), $F(\tau,x) = r_c^3 f$ is the dimensionless probability density in natural variables $\tau = t/t_{sep}$ and $x = r/r_c$, $\tau_d = t_d/t_{sep}$ is the dimensionless interpulse delay and $t_{sep} = r_c^2/D$ is the diffusion separation time of the pair.

The relationships (4.7) and (4.8) demonstrate the distinction between the kinetic PAIPS method and a pump-and-probe one based on the measurements of an optical absorption of geminate charges. In the latter case, as mentioned above, the time dependent absorption of geminate electrons and cations induced by the UV pulse is simply proportional to the geminate pair survival probability given by

$$W(t) = \int f(t,r)\, d^3r. \tag{4.9}$$

The distinction between the PAIPS and pump-and-probe experiments becomes most conspicuous in two limiting cases: $t_d \to \infty$ and $t_d \to 0$. From (4.7) and (4.8) follows that as $t_d \to \infty$ $\Delta q_1 \to 0$ and hence $\Delta Q \to 0$, whereas W tends to the dissociation probability q_0 at large times. On the other hand, as $t \to 0$ the enhancement Δq_1 depends, as seen from (4.8), on the initial distribution $f_0(r)$, whereas the survival probability $W \to 1$ at $t \to 0$ for any $f_0(r)$.

The relationship (4.7) has been extended [19] to the short IR pulse with the intensity u and duration $t_p \ll t_d$. At $u\sigma t_0 < 1$ the enhancement of the geminate pair dissociation probability is

$$\Delta q(\tau_d) = n\Delta q_1 = \frac{nL^2}{6r_c^2}\left(1 - \frac{T}{T_{ef}}\right) z(\tau_d), \tag{4.10}$$

where $n = u\sigma t_p = \Phi_{IR}\sigma/h\nu_{IR} s$ is the averaged number of successive photoexcitation events the electron undergoes repeatedly during the IR pulse. From Eqs. (4.2) and (4.10) we can write [19]

$$\frac{\Delta q}{q_0} = \frac{nL^2}{6r_c^2}\left(1 - \frac{T}{T_{ef}}\right) K(\tau_d), \tag{4.11}$$

$$K = z/q_0 = 4\pi\int_{R/r_c}^\infty x^{-2} F(\tau_d,x)\exp(-1/x)\, dx/q_0. \tag{4.12}$$

At $t_d \ll t_p$ the relationships (4.11) and (4.12) allow one to determine the dependence of $\Delta q/q_0$ on t_d provided that $f_0(r)$ is known.

Different kinds of distributions $f_0(r)$ are often used in ionization studies: exponential, δ-function

and Gaussian distribution [3,4,14,35,36]. Recently, the Gaussian form

$$f_0(r) = (\pi B^2)^{-3/2} \exp(-r^2/B^2) \qquad (4.13)$$

has been substantiated from theoretical point of view by Rips and Silbey [37] who showed that for the diffusion-like motion of quasi-free electrons, photogenerated under ionization in molecular media, the thermalization distance distribution function had the Gaussian form at large r.

For the Gaussian initial distribution (4.13) Eq. (4.1) was solved numerically and the probability density $f(t,r)$ was found. The curves in Fig. 5 depict the dependencies of K on τ_d obtained at different parameters $b = B/r_c$. As seen, at $\tau_d = t_d/t_{sep} > 0.1$ the function $K(\tau_d)$ weakly depends on b. As noted previously [14,18], this arises from the fact that at large times the distribution $f(t,r)/q_0$ weakly depends on the initial distribution $f_0(r)$. As can be seen from Fig. 5, at $t_d < 0.1 t_{sep}$ the decay kinetics $\Delta q(t_d)$ depends on B and therefore the parameter B can be determined by fitting the calculated curves $\Delta q(t_d, B)$ to the experimental dependence of ΔQ on t_d.

Fig. 6 demonstrates the functions $y = x^{-2} F(\tau, x) \exp(-1/x)$ in the right-hand side of (4.8) calculated at different $\tau = t/t_{sep}$ and two values of $b = B/r_c$. From (4.8) follows that $y(x)$ is proportional to the contribution from electrons at distance $r = xr_c$ to the Δq enhancement. At $L = 5$ nm and

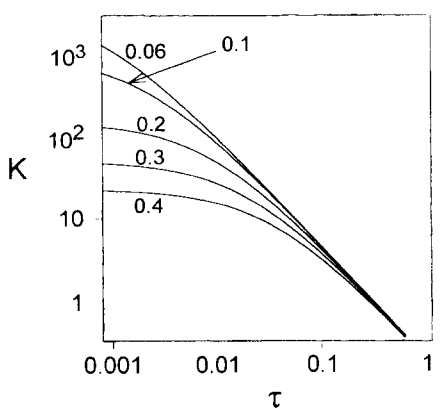

Fig. 5. The dependences of the parameter K given by (4.12) on the dimensionless time $\tau = t/t_{sep}$ calculated at different distances B of the initial Gaussian distributions. The numbers near the curves are $b = B/r_c$.

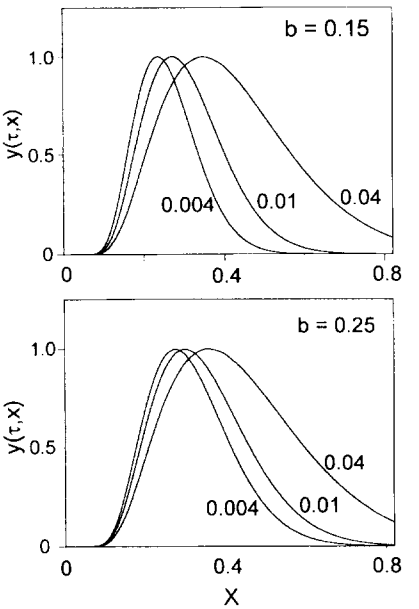

Fig. 6. The function $y(\tau,x)$ versus the radius $x = r/r_c$ worked out at $b = 0.15$ (top) and $b = 0.25$ (bottom). Numbers near curves are the times $\tau = tD/r_c^2$. Each curve has been normalized to unity at its maximum.

$r_c = 30$ nm the distances $r < L$ correspond to the region: $x < 0.17$. As seen from Fig. 6, the contribution from photoexcitation of geminate electrons with $x < 0.17$ to Δq is not more than 13% for $\tau = 0.004$ and much less than 10% for $\tau > 0.006$. This justifies approximation (4.4) at large time delays.

The relationship (4.5) can be extended to the case of finite UV and IR pulse durations, t_p, when t_p and t_d are of the same order of values. Let, at first, the pairs (e_t^-, A^+) be created at $t = 0$ followed by excitation by the long IR pulse. In the limit of $u\sigma t_0 \to 0$, $u(t)\sigma\Delta t$ is the average number of photoinduced localization events an electron undergoes during the time interval $(t,\ t+\Delta t)$. Therefore, under the assumption that (4.4) holds the function $f(t,r)$ satisfies the equation

$$\frac{\partial f}{\partial t} = D\left[\frac{\partial^2}{\partial r^2} + \left(\frac{2}{r} + \frac{r_c}{r^2}\right)\frac{\partial}{\partial r}\right] f + D_t\left[\frac{\partial^2}{\partial r^2} + \left(\frac{2}{r} + \frac{e^2}{\varepsilon k_B T_{ef} r^2}\right)\frac{\partial}{\partial r}\right] f, \qquad (4.14)$$

where $D_t = u(t)\sigma L^2/6$ is the light intensity dependent diffusion coefficient. The second member in the right-hand side of Eq. (4.14) describes the evolution of the trapped electrons spatial distribution due to photostimulated migration from one trap to another. The relationship (4.14) is seen to have the form of the Smoluchowski equation describing the motion of a charge particle with time dependent diffusion coefficient $D + D_t$ and temperature T_t given by

$$\frac{1}{T_t} = \frac{D}{D+D_t}\frac{1}{T} + \frac{D_t}{D+D_t}\frac{1}{T_{ef}}. \qquad (4.15)$$

It can be shown that as $u \to 0$ the contribution to Δq from the IR photons absorbed by trapped electrons during time interval $(t, t + dt)$ is

$$d(\Delta q) = \frac{\sigma u(t) z(t)\, dt L^2}{6 r_c^2}\left(1 - \frac{T}{T_{ef}}\right), \qquad (4.16)$$

where z is determined by the solution of Eq. (4.14) at $u = 0$. From (4.16) follows that in the case of finite pulse durations the value of $\Delta q/q_0$ is

$$\frac{\Delta q(t_d)}{q_0} = \frac{nL^2}{6r_c^2}\left(1 - \frac{T}{T_{ef}}\right)\int_{-\infty}^{\infty} g_1(t_1)\, dt_1 \int_{t_1 - t_d}^{\infty} \times g_2(t_2) K(t_d + t_2 - t_1)\, dt_2. \qquad (4.17)$$

Here $g_1(t)dt$ is that part of the pairs (e_t^-, A^+) which is created by the UV pulse in the time interval $(t, t + dt)$, $g_2(t) = u(t)h\nu_{IR}s/\Phi_{IR}$ is the time distribution function of the IR pulse intensity (both functions are normalized to unit: $\int g_k(t)dt = 1$, $k = 1,2$), s is the cross-sectional area of the IR laser beam, $n = \sigma \int u\, dt$. For our laser system the shape of $g_2(t)$ was found to be Gaussian: $g_2 = (1/\pi^{1/2}t_p)\exp(-t^2/t_p^2)$ with $t_p \approx 19$ ps [38]. The formula (4.17) was used to calculate the decay kinetics $\Delta q(t_d)$.

The validity of the convolution (4.17) was confirmed by the observed linear dependence of ΔQ on the intensity of the IR light. It should be emphasized that in the model under consideration the probability enhancement Δq must tend to a constant value with increasing the Φ_{IR} energy even at $u\sigma t_0 \ll 1$. Actually, one might expect the full photostimulated separation of the pair during the IR pulse when the pulse becomes sufficiently intense and long. In this case, the relationships (4.16) and (4.17) do not hold. However, the calculations presented in the Appendix show that at the used photons density a pulse $\Phi_{IR}/h\nu_{IR}s < 1.5 \times 10^{17}$ photon/cm^2, when the number of electron photoexcitation events is $n < 4$ per pulse, the deviation of the calculated dependence of Δq on Φ_{IR} from the linear law is small (not more than 20–30%). As shown in the Appendix, a great deal of the pairs are separated during the IR pulse only at $nL^2/6r_c^2 > 1$. This gives n > 200 which corresponds to a vastly greater IR laser intensity than that used.

5. Calculations and comparison with experiment

To find the time t_{sep}, the diffusion coefficient D was found as $D = mk_BT/e$ from the experimentally determined mobility of excess electrons m(cm^2 V^{-1} s^{-1}) = $105\exp(-2.16 \times 10^3/T)$ in methylcyclohexane [39]. The dielectric constant at low temperature was calculated from the Clausius–Mosotti equation using the temperature dependence of density of liquid MCH and the value of $\varepsilon = 2.02$ at $T = 293$ K [40]. The time t_{sep} varies in magnitude from 4.5 ns at 293 K up to 118 ns at 220 K.

Since the model presented above is valid at rather large times ($> 0.003t_{sep}$), the comparison between the decay kinetics calculated from Eqs. (4.11) or (4.17) and experimental one was performed in the following way. At each temperature we first chose a fixed time delay $t^* > 0.003t_{sep}$ and then fitted the calculated decay curves $\Delta q(t_d, B)$ to experimental one $\Delta Q(t_d)$ only at $t > t^*$, see Figs. 3 and 7. Each curve in Fig. 3 and Fig. 7 has been normalized to unity at $t_d = t^*$. Since the interpulse delay in our experiments was not more than 1.3 ns, the fitting was made only at rather large temperatures (> 245 K) at which $t_{sep} < 30$ ns and hence the range of t_d between t^* and maximum possible t_d was large enough. Some parameters used in such the calculations for the solutions of anthracene are presented in Table 1.

The values of B obtained are plotted in Fig. 8 versus the excess energy, ΔE, of the solute above its ionization threshold. As seen, the distance B varies in magnitude from 4.5 ± 1 nm for anthracene at $\lambda_{UV} = 360$ nm up to 10 ± 1.5 nm for TMPD at $\lambda_{UV} = 270$ nm.

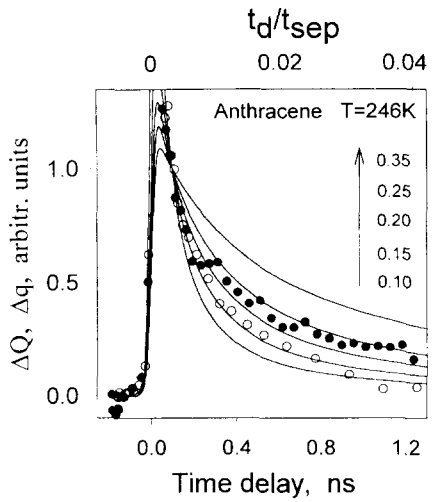

Fig. 7. Comparison between the experimental decay kinetics $\Delta Q(t_d)$ observed in the solution of anthracene at 246 K (points) and the curves $\Delta q(t_d)$ calculated from Eq. (4.17). Open points $\lambda_{UV} = 360$ nm, filled points $\lambda_{UV} = 270$ nm. Each curve has been scaled to unit at $t_d = t^* = 98$ ps. The numbers near the vertical arrow are the parameters $b = B/r_c$ corresponding to calculated curves. The upper scale shows $\tau_d = t_d/t_{sep}$. The used parameters are: $\varepsilon = 2.094$, $r_c = 32.2$ nm, $D = 3.4 \times 10^{-4}$ cm^2 s^{-1} and $t_{sep} = 31$ ns.

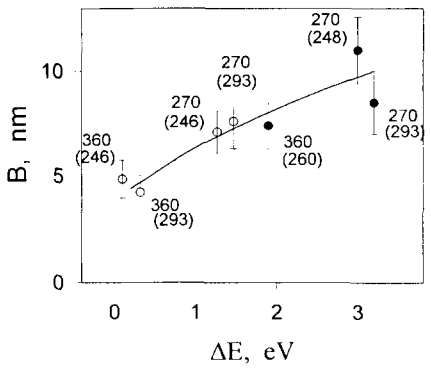

Fig. 8. The measured initial separation B in the geminate pair (e_t^-, A^+) versus the excess excitation energy obtained from Eq. (6.7). Open points anthracene, filled points TMPD. The numbers near points are the wavelengths of the UV radiation, the numbers in brackets are the temperature.

It is worth noting that the obtained separation B weakly depends on t^*. Moreover, the convolution (4.17) for the Gaussian forms of g_1 and g_2 with $t_p = 19$ ps permits us to describe the overall experimental curve $\Delta Q(t_d)$ including the rise kinetics at $t_d < 0$, the peak and the decay kinetics up to $t_d = 1.3$ ns. The magnitude of B resulting from such fitting is only by 10–25% less that obtained from fitting at $t_d > t^*$. Such an agreement between calculated and experimental curves arises from the fact that at short $t_d < 0.001 t_{sep}$ when, strictly speaking, the diffusion model is not valid the time dependence $K(t_d)$ is rather smooth, especially at large B (see Fig. 5).

Table 1
The parameters used in fitting of the experimental decay curves $\Delta Q(t_d)$ for the solutions of anthracene and the distances B obtained

λ_{UV} (nm)	T (K)	r_c (nm)	t_{sep} (ns)	t^* (ns)	B (nm)
360	293	28.2	4.5	0.045	4.2 ± 0.9
360	246	32.4	31	0.100	4.8 ± 1
270	293	28.2	4.5	0.045	7.6 ± 1.4
270	246	32.4	31	0.100	7.1 ± 1

The comparison of the measured enhancement $\Delta Q/Q$ with Eqs. (4.11) and (4.17) yielded the length $L(1 - T/T_{ef})^{1/2} \approx 3.5$–$4.2$ nm at $\sigma = 3 \times 10^{-17}$ cm^2 [31]. This gives $T_{ef} = 730 \pm 60$ K and $L = 4.8 \pm 0.4$ nm at $\Delta_e = 6 \times 10^{-13}$ cm^2/V. The obtained parameters are less than the earlier estimated values of $T_{ef} \approx 1000$ K and $L = 6$ nm [19,21]. A possible reason for the discrepancy is the nonhomogeneous intensity distribution in the cross sectional area of laser beams. Really, the Eqs. (4.11) and (4.17) are valid only if both laser beams or, at least, one of them (UV or IR) is homogeneous. Although the incomplete coincidence between the high intensity areas of the UV and IR laser beams is unlikely to affect the observed decay kinetics $\Delta Q(t_d)$, it can diminish ΔQ resulting in smaller measured values of L and T_{ef}.

6. Discussion

6.1. Nature of the optical absorption of trapped electrons

The obtained high effective temperature $T_{ef} > T$ suggests the creation in reaction (1.1) of nonthermalized (hot) electrons as for a bound–free electron transition. It should be noted that the nature of

optical transitions for trapped electrons in hydrocarbon liquids and glasses is not fully clear. Some workers have interpreted the optical absorption spectra of e_t^- as arising entirely from a bound–free transition [41–43], while the other workers have assigned portions of the spectra to bound–bound and bound–free transitions [44–48].

It is commonly supposed that a distinction between bound–free and bound–bound transitions can be made by comparison of the dc photoconductivity and the optical spectra versus photon energy [44–47]. A coincidence of forms of these spectra in γ-irradiated MCH glass and a large measured quantum yield 0.8 ± 0.4 of photogeneration of the quasi-free electron in reaction (1.1) have allowed Novikov and Yakovlev [43] to assign the observed electron spectra to bound–free transition. For other systems, like 3-methylpentane (3-MP) and 2-methylpentane glasses, the discrepancy between photoconductivity and absorption spectra observed near an electron photoionization threshold (i.e. at $h\nu < 1$–1.3 eV) has been interpreted as the coexistence of bound–bound and bound–free transitions the former being predominant [46,47]. The coincidence of these spectra at $h\nu > 1.5$ eV has been interpreted as bound–free transition [47].

Such an approach is based on the assumption that for a bound–free electron transition the contribution to the dc photoconductivity signal from a photon absorption by an electron e_t^- does not depend on the position of e_t^- and on the thermalization length, L_{hot}, of quasi-free hot electrons created in reaction (1.1). It is the case only for photoexcitation of free electrons which are not bound by the Coulombic centre. The photoexcitation of free electrons seems to make a main contribution to the photocurrent observed in MCH glass, while in 3-MP glass the photocurrent was induced mainly by excitation of geminate trapped electrons [5]. Recently, Yakovlev has studied the kinetics of photoconductivity induced by excitation of geminate electrons in 3-MP glass, assuming that optical absorption of e_t^- is due to the bound–free transition [6]. It has been shown that the contribution to the dc photocurrent from each photon absorbed by a trapped electron e_t^- depends both on the distance r and on the thermalization length L_{hot} of e_{hot}^- (here r is the distance between e_t^- and its parent cation) [6]. On the other hand, the length L_{hot} in its turn strongly depends on $h\nu$ at $h\nu < 1$ eV [5]. Thus, Yakovlev has concluded [6] that the spectral dependence of photocurrent in 3-MP glass normalized to the e_t^- absorption rate is not independent of $h\nu$ even if the photoionization quantum yield of e_t^- is equal to unity. Therefore the conclusions about bound–bound transitions in alkane glasses at $h\nu <$ 1–1.3 eV [47], based on the discordance between the photocurrent and absorption spectra, can be in error. Moreover, the assumption that electron absorption is due to bound–free transition is consistent with a great body of experimental data obtained for γ-irradiated 3-MP glass: the measurements of photoassisted free ion radiation yield [5,49], radiation yield of trapped electrons [5,6,49], quantum yield of photostimulated geminate electron recombination [49], an experimentally determined amplitude and kinetics of photoconductivity induced by excitation of geminate trapped electrons [6,49]. It seems likely that the bound–free electron transition in a photon absorption by e_t^- is rather common for all alkane glasses and liquids because optical spectra of e_t^- are well similar for them.

6.2. Thermalization and localization of low energy electrons in liquid methylcyclohexane

Although the high effective temperature of e_{hot}^- obtained agrees with the creation of nonthermalized electrons in reaction (1.1), it should be emphasized that, in order to find the effective temperature T_{ef}, we have not taken assumptions on the nature of the electron transition as a starting point for determining T_{ef}. In particular, T_{ef} does not depend on the value of σ used. In fact, the measurements of $\Delta Q/Q$ and Φ_{IR} have allowed us to find the value of $\sigma L^2(1 - T/T_{ef})$ from (4.11) or (4.17). On the other hand, the product $\sigma\Delta_e$ has been determined from the measurements of the dc photocurrent transients arising from the photoexcitation of e_t^-, after that the value of Δ_e has been obtained, assuming that σ equals the absorption cross section of e_t^- [21,32]. Thus, the ratio L^2/Δ_e and hence T_{ef}, found from these two sorts of measurements, is independent of σ. Nevertheless, the length $L = 4.8 \pm 0.4$ nm, obtained above at $\sigma = 3 \times 10^{-17}$ cm^2 as in the case of a bound–free transition, coincides with the thermalization length $L_{hot} \approx$ 5 nm at $h\nu = 1.2$ eV, determined by Yakovlev [5] in

3-MP glass where the bound–free electron transition was consistent with a great body of experimental data [5,6,49]. This provides an additional support for the assumption that the optical absorption of electrons at 1080 nm in liquid MCH, as well as in MCH [43] and 3-MP [5,6] glasses, is due to a bound–free electron transition. In this case, the measured parameters T_{ef} and L should be assigned to a hot electron with the initial kinetic energy $E_{ini} = h\nu_{IR} - E_{tr} = 0.83 \pm 0.14$ eV where $h\nu_{IR} = 1.15$ eV and the optical depth, E_{tr}, of the electron trap is taken to be between the activation energy 0.19 eV of excess electron mobility in liquid MCH [39] and the photoionization threshold 0.44 eV of trapped electrons in MCH glass [43].

For low energy photoelectrons in hydrocarbon liquids the direct measurements of electron thermalization and localization rates in pump-and-probe experiments seems to be hampered by the contribution at short times $t < 1$ ps to the absorption signal from neutral excited states [7,8,12,13]. However, the measured effective temperature and drift displacement of e^-_{hot} in liquid MCH allow us to estimate the full localization time t_0 of e^-_{hot} and the diffusion distance traveled by the electron after its thermalization until the formation of the stable trapped state e^-_t occurs. These estimates justify the diffusion approach used above to describe geminate recombination of the pair (e^-_t, A^+), at least, at times longer than 1 ps after the electron injection into the liquid.

We shall not consider all the models for thermalization of low energy electrons in hydrocarbon media discussed in different works [33,34,37,50–53]. We evaluate, at first, the ratio of the mean squared thermalization distance to the drift displacement of electron within a simple thermalization picture of Mozumder and Magee [50] in which the electron travels the main part of thermalization distance when its energy becomes less than the threshold of C–H stretching vibrations $E_{vib} = 0.4$ eV. We suppose with Balakin and Yakovlev [54] that at energy $E < E_{vib}$ the electron suffers a large number M of elastic scattering events when its energy relaxes from E_{vib} down to an energy, E_{th}, of the order of thermal one. Assuming that an elastic scattering mean free path, λ_{el}, of the electron and its average energy loss, δE, per one act of elastic scattering are independent of the energy E, the drift displacement in an unit electric field of the hot electron, created in reaction (1.1), during its thermalization can be estimated as [14,54]

$$\Delta_{hot} = \frac{e}{2m}\sum_{i=1}^{M}\frac{\lambda_{el}^2}{v_i^2} = \frac{e\lambda_{el}^2}{4\delta E}\sum_{i=1}^{M}\frac{\delta E}{E_i}$$

$$\approx \frac{e}{4}\frac{M\lambda_{el}^2}{(E_{vib}-E_{th})}\ln\left(\frac{E_{vib}}{E_{th}}\right), \qquad (6.1)$$

where $\delta E = (E_{vib} - E_{th})/M$, m is the electron mass, v_i and $E_i = mv_i^2/2$ are its velocity and energy corresponding to the ith act of elastic scattering. Since the mean squared thermalization distance of e^-_{hot} equals $L^2_{hot} = M\lambda^2_{el}$, we can define the temperature of the hot electron in the thermalization process by the equation [19]

$$T_{hot} = \frac{eL^2_{hot}}{6k_B\Delta_{hot}} = \frac{2}{3}\frac{(E_{vib}-E_{th})}{k_B\ln(E_{vib}/E_{th})}$$

$$= 1060\text{–}1200\,\mathrm{K} \qquad (6.2)$$

at $E_{th} = 3k_BT/2$ and $T = 200$–290 K. Such a value of T_{hot} coincides within a factor of two with T_{ef} in liquid MCH. This confirms the creation of nonthermalized electrons in reaction (1.1). Moreover, basing on the experimentally determined values of L and Δ_e, it has been concluded that the localization of hot electrons in liquid MCH and n-hexane, opposite to more viscous squalane and 3-MP glass, occurs before or just after their thermalization [14,19,20,54]. At $E_{ini} > k_BT$ these parameters can be presented as the sum of values corresponding to the motion of the electron before and after thermalization [14,20,54]:

$$L^2 = L^2_{hot} + L^2_0, \qquad (6.3)$$

$$\Delta_e = \Delta_{hot} + m_0t_0, \qquad (6.4)$$

where $L^2_0 = 6m_0t_0k_BT/e$ is the mean squared diffusion length of the thermalized mobile (quasi-free) electron, m_0 and t_0 are its mobility and full solvation time, respectively. Here we assume the existence in the scheme (1.1) of mobile thermalized precursor of the equilibrated trapped electron e^-_t with mobility m_0 and diffusion length L_0. Inserting $\Delta_e = eL^2/6k_BT_{ef}$ and $\Delta_{hot} = eL^2_{hot}/6k_BT_{hot}$ into (6.4) and using $T/T_{hot} \ll 1$, the lengths L_{hot} and L_0

can be obtained from the following relationships [20]:

$$L_{hot}^2 \approx L^2\left(1 - \frac{T}{T_{ef}}\right), \tag{6.5}$$

$$L_0^2 \approx L^2\left(\frac{T}{T_{ef}} - \frac{T}{T_{hot}}\right) = \frac{6k_B\Delta_e T}{e}\left(1 - \frac{T_{ef}}{T_{hot}}\right). \tag{6.6}$$

For 3-MP glass and squalane the diffusion length $L_0 = 4.5$ nm has been reported [5,20]. For liquid MCH, using $\Delta_e = 5 \times 10^{-13}$ cm^2 V^{-1} at 200 K [32], we obtain from (6.6) that $L_0 < (6k_B T\Delta_e/e)^{1/2} = 2.2$ nm even if $T_{ef} \ll T_{hot}$. This gives $m_0 t_0 < 4 \times 10^{-13}$ cm^2 V^{-1}.

A more lesser diffusion length $L_0 < 1$ nm for liquid MCH can be inferred from (6.6) at $\Delta_e = 5 \times 10^{-13}$ cm^2 V^{-1}, if it takes into account that the high effective temperature T_{ef} measured is close to the proposed value of T_{hot}. A similar evaluation $L_0 < 1.8$ nm was obtained in Refs. [14,32] from the comparison between the measured drift displacement Δ_e in liquid MCH and the calculated magnitude of Δ_{hot}. It should be emphasized that, in order to make an estimate of L_0, we have used only the experimental values of Δ_e and T_{ef} and the assumption that $T/T_{hot} \ll 1$ which is likely to hold within any thermalization model for electrons with initial energy ~ 1 eV.

From $m_0 t_0 < 4 \times 10^{-13}$ cm^2 V^{-1} it follows that the electron localization time $t_0 < 0.4$ ps at a reasonable mobility of quasi-free electrons $m_0 > 1$ cm^2 V^{-1} s^{-1}. Small time t_0 is confirmed by the observed linear dependence of ΔQ for the solutions of anthracene on the energy Φ_{IR}, at least, up to $\Phi_{IR} \approx 3$ mJ that corresponds to the condition $u\sigma t_0 < 1$ at $t_0 < 3.7$ ps where $u = \Phi_{IR}/h\nu_{IR} t_p s$ is the light intensity of the IR laser pulse. In addition, the comparison between initial separation distances B within ion pairs, obtained at different temperatures (see Table 1), provides support for the assumption that t_0 is not more than a few picoseconds in liquid MCH. Really, at $T = 246$ K the diffusion separation time t_{sep}, as seen in Table 1, is rather large (31 ns). Because of this, the experimental curves $\Delta Q(t_d)$ were fitted to the calculated curves $\Delta q(t_d)$ at rather large $t_d > t^* = 100$ ps, i.e. at $t_d \ll t_p \approx 20$ ps. In this case, Δq is simply proportional to $K(t_d)$ even if $t_0 > t_p$. (At $t_0 \ll t_p$ the relation between $\Delta q(t_d)$ and $K(t_d)$ is given by (4.11).) Therefore, the parameter B, found by the fitting at $T = 246$ K, has weakly depended on t_0/t_p. At room temperature, as can be seen in Table 1, $t^* \approx 2t_p$ and hence, to fit the kinetic curves, we used the convolution (4.17) which was valid only at rather small solvation times t_0: at $t_0 \ll t_p \approx 20$ ps and at $t_0 < (u\sigma)^{-1} \approx 4$ ps for $\Phi_{IR} = 3$ mJ. However, the values of B obtained at 246 and 293 K are seen to be close to each other. (Moreover, as noted above, the convolution (4.17) allows one to describe the overall observed curve $\Delta Q(t_d)$ including both the rise kinetics at $t_d < 0$ and the decay at $t_d > 0$.) This confirms the assumption that t_0 is of the order of 1 ps.

As noted previously [14,20,32,54], the diffusion length $L_0 < 1$–2 nm is too small for the quasi-free state for which one should expect that $L_0 > \lambda_{el} > \kappa^{-1}$ where $\kappa = (2mk_B T)^{1/2}/\hbar = 1.5$ nm is the wave number for a thermal electron. Using such arguments, it has been concluded that in low electron mobility liquids, like n-hexane or MCH, the electrons with energy of the order of 0.01 eV are captured by shallow traps and then stabilized there because of the fast reorganization of the liquid around the initial trapping sites [14,20]. Thus, in liquid MCH the parameters L and Δ_e are determined mainly by the thermalization rate: $L_0 \approx 0$, $L = L_{hot}$ and $\Delta_e = \Delta_{hot}$ [20]. In such a localization picture, the full solvation time t_0 of e_{hot}^- seems to be close to its thermalization time. This agrees with the conclusion made above that t_0 does not exceed a few picoseconds in liquid MCH.

The small t_0 and L_0 justify the use of the Smoluchowski equation (4.1). Actually, in an often-used two state model for the excess electron transport in liquid alkanes the electrons are assumed to be partially quasi-free and partially trapped [55,56]. Such the model requires the diffusion length of thermal quasi-free electrons to be rather large: $L_0 > \lambda_{el} > \kappa^{-1}$. As noted in Ref. [54], the small L_0 in liquid n-hexane and MCH suggests that for these liquids the use of the two state model is hardly justified. It seems likely that in the absence of photoexcitation the electron jumps from one trap to another without formation of a conducting state. The mean distance

of jumps is expected to be of the order of a molecular size. Even if the thermal activation promotes an electron from the trap into a conducting state, the electron suffers not more than a few scatterings with $L_0 < 1$–2 nm until retrapping occurs. Thus, Eq. (4.1) is a reasonable approximation to describe geminate recombination of the pairs (e_t^-, A^+) in liquid MCH, at least, at $t > 1$ ps after the injection of electron into the liquid and at the distances $r > 2$ nm between the partners of the pair. As to the pairs (e_t^-, A^+) with small distances $r < 3$ nm, their dissociation probability is less than $\exp(-r_c/r) < 10^{-4}$ at room temperature ($r_c = 28.3$ nm). Therefore, the contribution of these pairs to the free ion current in the solutions of anthracene and TMPD can be ignored because the obtained distances B in Fig. 8 correspond to much larger dissociation probability $q_0 > 5 \times 10^{-3}$ at room temperature.

6.3. Mechanism of photoionization of aromatic solutes

Under the assumption that the second photon of the UV laser is absorbed by the relaxed singlet state S_1 of the solute molecule the initial excitation excess energy of the solute, plotted as abscissas in Fig. 8, has been found as

$$\Delta E = h\nu_{UV} + E_S - IP_{liq}, \tag{6.7}$$

where E_S is the energy of the S_1 state (3.3 eV for anthracene and 3.46 eV for TMPD [30]), IP_{liq} is the photoionization potential of the solute in liquid and $h\nu_{UV}$ is the energy of the UV photon. The values of IP_{liq} at different temperatures have been determined from photoconductivity measurements [14,57]. For TMPD in MCH we used $IP_{liq} = 4.83$ eV at 296 K (average between 4.82 eV [58] and 4.85 eV [59]) and $\partial IP_{liq}/\partial T = -4 \times 10^{-3}$ eV/K [59].

To determine IP_{liq} for anthracene, we used the relation between IP_{liq} and the electron conduction band energy V_0 in liquid [57,60]

$$IP_{liq} = IP_g + V_0 + G \tag{6.8}$$

where IP_g is the ionization potential of solute molecule in gas, $G = -e^2(1 - 1/\varepsilon)/2R_{cat}$ is the polarization energy of anthracene cation, R_{cat} is its radius. From (6.8) follows that the ionization potential of anthracene in methylcyclohexane IP_{MCH} at 293 K can be found from the relationship

$$IP_{MCH} = IP_{TMP} + V_0(MCH) - V_0(TMP) + \frac{e^2}{2R_{cat}}\left(\frac{1}{\varepsilon_{MCH}} - \frac{1}{\varepsilon_{TMP}}\right), \tag{6.9}$$

where $IP_{TMP} = 6.14$ eV is the one-photon ionization potential of anthracene in 2,2,4-trimethylpentane at 293 K determined from photoconductivity measurements [61], $\varepsilon_{MCH} = 2.02$ and $\varepsilon_{TMP} = 1.943$ are dielectric constants of MCH and 2,2,4-trimethylpentane, respectively [39], $V_0(MCH) = 0.08$ eV [58] and $V_0(TMP) = -0.24$ eV [62] are the conduction band levels for excess electrons in liquid MCH and 2,2,4-trimethylpentane, respectively. This gives the estimate of $IP_{MCH} = 6.42$ eV at $T = 293$ K and $R_{cat} = 0.325$ nm [61]. For anthracene the temperature dependence of IP_{liq} is not known. So at $T < 293$ K we used the value $\partial IP_{liq}/\partial T = -4 \times 10^{-3}$ eV/K as well as for TMPD in MCH. (This results in an uncertainty of IP_{liq} not more than 0.05 eV at $T > 240$ K.)

The observed increase of the initial separation B with increasing excess energy ΔE, shown in Fig. 8, suggests the existence in reaction (1.2) of the quasi-free hot electrons e_{hot}^-, the immediate precursors of e_t^-, which are injected following the photoionization of the aromatic molecules with an initial kinetic energy that increases with increasing ΔE.

It should be emphasized that the use of the ΔE parameter alone is unlikely to be sufficient to encompass all variables in the geminate escape problem. For example, both $f_0(r)$ and electron escape probability are expected to depend on the shape of the initial photoelectron kinetic energy distribution. In particular, the prompt relaxation of a highly excited state A^* in scheme (1.2) can reduce the initial kinetic energy of the photoelectrons e_{hot}^- and affect the shape of the energy distribution. However, for the systems under investigation the autoionization of the state A^* is likely to be more prompt than its relaxation. In this case, the hot photoelectron carries away the bulk of the excess energy ΔE. Such a simple photoionization mechanism agrees with the temperature dependence of photocurrent induced in the solutions of anthracene and TMPD by the UV pulse acting alone. We have measured the activation

energy of the UV induced photocharge and have compared it with the activation energy, E_a, of the geminate pair dissociation probability q_0 [63]. It has been shown that E_a can be expressed in terms of the parameters B and dB/dT [63]. If it takes into account the existence in reaction (1.2) of the hot electron which undergoes elastic and inelastic scatterings during its thermalization, the derivative dB/dT can be presented as [63]

$$\frac{dB}{dT} = -\frac{B}{\rho_0}\frac{d\rho_0}{dT} + \frac{\partial B}{\partial IP_{liq}}\frac{\partial IP_{liq}}{\partial T}, \qquad (6.10)$$

where ρ_0 is the density of liquid. The first member in the right-hand side of (6.10) corresponds to the increase of the electron scattering centre concentration with cooling and the second member describes the contribution from the proposed temperature dependence of the initial energy, ΔE, of e^-_{hot} which in its turn is expected to decrease with cooling because $\partial IP_{liq}/\partial T < 0$ [59] and hence $\partial(\Delta E)/\partial T > 0$. If the electron e^-_{hot} in the scheme (1.2) carries away all the excess excitation energy ΔE, $\partial B/\partial IP_{liq}$ can be roughly estimated from the slope of the plot of B versus ΔE in Fig. 8 as $\partial B/\partial IP_{liq} = -\partial B/\partial(\Delta E)$. This gives $dB/dT \approx 0.01$–0.02 nm/K [63]. Calculations show [63] that the distances B presented in Fig. 8 together with dB/dT, estimated from (6.10), correlate with the measured activation energy E_a that provides support for generation of hot electrons in photoionization of aromatic solutes.

In Fig. 8, the values of B, obtained at different temperatures between 246 and 293 K, are given solely as a function of the energy ΔE. This is justified if B weakly depends on T. It is expected that $dB/dT \approx 0.01$–0.02 nm/K [63]. For such dB/dT the proposed change of the parameter B in the temperature range of 240–293 K $\Delta B \approx 0.5$–1 nm is too small in order to be measured by the kinetic technique with accuracy we used. As to lower temperatures, although the large values of $\Delta Q/Q$ can be reliably measured at low temperatures (see Fig. 1b), at $T < 240$ K the diffusion separation time is too large $t_{sep} > 40$ ns and hence the important range in time delays of 0.04–0.5 ns, we used in fitting experimental curves, corresponds to small dimensionless delays $t_d/t_{sep} < 0.01$ for which the diffusion approach described above is not applicable, see Fig. 1b.

The increase of the initial separation B with increasing ΔE has been observed previously for the case of one photon ionization of TMPD in hydrocarbon solutions [64]. It seems likely that once the ionization energy of solute molecules in liquid is exceeded, the autoionization of initially excited states A^* becomes much more prompt than their relaxation. The excess energy carried away by the injected electron determines the distance B. The assumption that the autoionization is prompt does not contradict the observed fast rise time ($< 10^{-11}$ s) of the PAIPS signal measured as a function of time delay. Contrary to a delayed photoionization of large molecules and atomic clusters, like C_{60}, the prompt electron departure on a time scale $< 10^{-14}$ s is rather common for most small ionized molecules examined so far in gas phase [65]. Nevertheless, it should be mentioned another possible picture of the electron photogeneration. In p-terphenyl crystals the weak dependence of carrier generation quantum yield on the energy of the excitation [66] has been attributed to an electron injection from rapidly relaxed lower-lying states A^* which autoionizes, irrespectively of the value of the initial excitation energy. For such mechanism, the distance B would be expected to be independent of ΔE.

In conclusion, it is interesting to compare the kinetic PAIPS method with pump-and-probe one. It has been noted [12,13] that the chief problem in the picosecond transient absorption measurements of geminate electron–cation recombination is the excited neutral state absorption at the wavelength of the probe beam. As to the IR enhanced conductivity signal, the contribution from the two-photon ionization of the singlet states of the solute to the PAIPS signal can be reduced by decreasing the intensity and increasing the wavelength of the IR light.

Because of the high sensitivity of the conductivity technique, the PAIPS method allows one to study the mechanism of neat two-photon ionization of the solute at low energy density in the UV pulse $\Omega_{UV} <$ 0.01–0.1 mJ/cm^2 while the transient absorption measurements need usually much more value of $\Omega_{UV} \approx 10$–10^2 mJ/cm^2. (But it requires less the IR pulse intensity, opposed to the PAIPS technique.) In the case of absorption measurements, the perturbation of the initial geminate pair spatial distribution and free ion yield by the absorption of the third UV

photon by a geminate electron, as noted [13], becomes possible at such large Ω_{UV} even if the optical cross section of the electron at the wavelength of the UV pump beam is 10^{-18}–10^{-17} cm^2. Taken together, all these factors make the kinetic PAIPS technique to become, in addition to the optical absorption measurements, the promising tool for studies initial stages of ionization in liquids.

7. Summary and concluding remarks

A laser time-resolved picosecond PAIPS technique is discussed for studding initial stages of photoionization in hydrocarbon liquids. The kinetics of geminate recombination of the pairs (e_t^-, A^+), produced by two-photon ionization of anthracene and TMPD in liquid methylcyclohexane with the UV pulses at 360 or 270 nm, has been investigated by this technique in order to explore the effect of the initial excitation energy of aromatic solutes on the initial separation distance B within the geminate pair (e_t^-, A^+). For solutions of TMPD the slow component of the decay curves $\Delta Q(t_d)$ has been observed which is attributed to two-photon ionization of the TMPD singlets by the IR pulse. The IR enhanced photocharge ΔQ, observed in the solutions of anthracene, and the prompt component of the curves $\Delta Q(t_d)$ in the solutions of TMPD have been assigned to formation of nonthermalized (hot) electrons in an IR photon absorption by an electron. Within the diffusion model of the photostimulated ion pair dissociation [19,21] the time evolution of the spatial distribution $f(t,r)$ of the pair (e_t^-, A^+) has been analyzed and the effect of the IR laser pulse intensity on $f(t,r)$ has been investigated in order to develop in the picosecond time regime the procedure of fitting experimental decay curves $\Delta Q(t_d)$ to calculated ones, including the convolution over finite pulse durations at short interpulse delays. The distances B, found in the systems under investigation, suggest the prompt injection into the liquid of hot electrons in the UV ionization of aromatic solutes. Comparison has been made of the pump-and-probe method generally adopted with the PAIPS that used in the investigation.

It should be noted that the use of the Smoluchowski equation (4.1) for describing electron–cation recombination in the absence of electron photoexcitation is justified for the low electron mobility liquids, like MCH or n-hexane, in which the fast electron localization makes the diffusion length L_0 of quasi-free electrons small. In the "middle electron mobility" hydrocarbon liquids (with the excess electron mobility $m = 1$–10 cm^2 V^{-1} s^{-1}) the lesser efficiency of electron localization seems to result in the larger diffusion lengths of thermal quasi-free electrons. For example, a rather large length $L_0 = 18 \pm 3$ nm was reported [67] for liquid 2,2,4-trimethylpentane at 175 K ($m = 1.7$ cm^2 V^{-1} s^{-1}). For such large L_0 the geminate pair recombination can occur through both conducting and trapped electron states. Within the two-state model for electron transport the rate of geminate recombination at large L_0 is given, instead of (4.1), by the system of equations describing the time dependence of distribution functions for quasi-free and trapped electrons [68]. In the middle mobility liquids the enhancement of free ion yield due to geminate electron photoexcitation has not been observed yet. Since at $m = 1$–10 cm^2 V^{-1} s^{-1} the time interval $(10^{-3}$–$10^{-2})r_c^2/D$ of maximum values of $\Delta Q/Q$ in Fig. 5 corresponds to the range in time delays of 0.04–4 ps, one might expect that the effect of photoassisted ion pair separation will be revealed in these liquids in the subpicosecond domain. On the other hand, at such short times the electron photoexcitation by the IR pulse is expected to compete with primary electron localization. Thus, the further subpicosecond PAIPS experiments will give a new information about both geminate recombination and localization of photoelectrons in molecular liquids.

Acknowledgements

We would like to thank Dr. E. Rubtsova for assistance and technical service and Dr. A.A. Balakin for useful discussions. The research described in this publication was made possible in part by Grant No. JAX100 from the International Science Foundation and Russian Government and in part by Grant No. 93-03-05254 from the Russian Foundation for Fundamental Research.

Appendix A

To establish a range of the IR light energy (Φ_{IR}) in which the enhancement of escape probability Δq is linear with Φ_{IR}, below we compute Δq as a function of Φ_{IR} in the simple case of the IR pulse with a stationary light intensity:

$$u(t) = u_0 = \text{const}, \quad \text{at } t_d < t < t_d + t_p$$
$$= 0, \quad \text{at } t < t_d \text{ and } t > t_d + t_p \tag{A.1}$$

where t_p is the pulse duration. The pair (e_t^-, A^+) is assumed to be created at $t = 0$. We have considered that at $t < t_d$ and $t > t_d + t_p$ the probability density $f(t,r)$ satisfies Eq. (4.1) and at $t_d < t < t_d + t_p$ it satisfies Eq. (4.14) with constant coefficient $D_t = u_0 \sigma L^2/6$. The equations were solved numerically and the IR induced probability enhancement was found as $\Delta q/q_0 = (q_1 - q_0)/q_0$ where the IR enhanced escape probability q_1 was obtained from

$$q_1 = \int f(t_d + t_p, r) P(r)\, d^3 r. \tag{A.2}$$

For a given parameter B of the initial distribution and fixed times t_d and t_p the value of $\Delta q/q_0$ is determined, as seen from (4.14), by T_{ef}/T and nL^2/r_c^2 only (here $n = u_0 \sigma t_p$). From (4.14) it follows that at $n \to 0$ the $\Delta q/q_0$ enhancement is linear with n:

$$\frac{\Delta q}{q_0} = \frac{nL^2}{6r_c^2}\left(1 - \frac{T}{T_{ef}}\right)\frac{1}{t_p}\int_0^{t_p} K(t_d + t)\, dt. \tag{A.3}$$

At $n \to \infty$ the $\Delta q/q_0$ enhancement tends to the maximum value $(\Delta q/q_0)_{max} = (q_1^m - q_0)/q_0$ where q_1^m is the greatest possible IR enhanced escape probability of the pair given by

$$q_1^m = \int f(t_d, r) \exp\left(-\frac{e^2}{\varepsilon k_B T_{ef} r}\right) d^3 r. \tag{A.4}$$

Fig. 9 demonstrates how the IR pulse with $nL^2/6r_c^2 = 0.2$ affects the decay kinetics of the geminate pair survival probability $W(t)$ given by (4.9). For MCH at room temperature the parameters b, $\tau_d = t_d/t_{sep}$ and $\tau_p = t_p/t_{sep}$, chosen in calculating in Fig. 9, correspond to $B \approx 4.5$ nm, $t_d \approx 45$ ps and $t_p \approx 23$ ps. In the absence of the IR illumination the probability W is seen to approach from above to escape

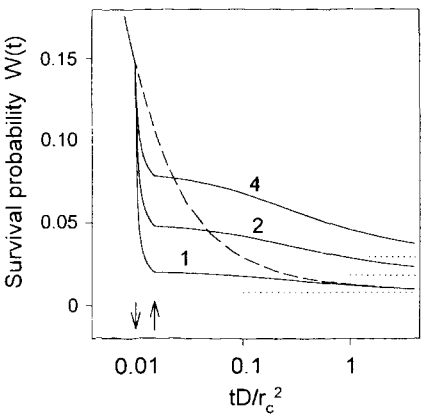

Fig. 9. The time dependence of geminate pair survival probability in the darkness (dashed line) and under the IR pulse action at $nL^2/6r_c^2 = 0.2$ (solid lines 1, 2 and 4). The ratio T_{ef}/T was taken to be: 1 (curve 1), 2 (curve 2) and 4 (4). The used parameters are: $b = 0.15$, $t_d = 0.01 t_{sep}$ and $t_p = 0.005 t_{sep}$. The arrows indicate the onset and completion of illumination. The horizontal dotted lines show the escape probabilities q_0 and q_1 calculated from Eqs. (4.2) and (A.2), respectively.

probability q_0 at $t \to \infty$. The chosen value of $nL^2/6r_c^2 = 0.2$ corresponds to rather large $n \approx 43$ at $L = 5$ nm and $r_c = 30$ nm. The electron photoexcitation results, as seen from Fig. 9, in the increase of escape probability (at $T_{ef} > T$) and the decrease of $W(t_d + t_p)$ arising from the photostimulated geminate recombination during the IR pulse. The difference $W(t_d) - W(t_d + t_p)$ is seen to decrease with

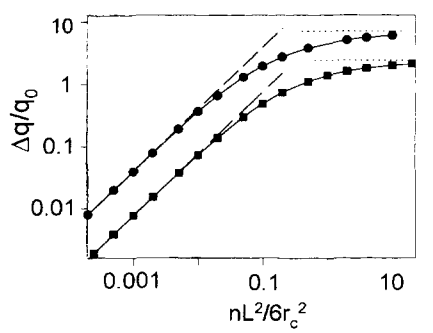

Fig. 10. The relative increase of a geminate pair dissociation probability versus $nL^2/6r_c^2$ (points) obtained at the following parameters: $b = B/r_c = 0.15$, $T_{ef}/T = 4$ and $t_p = 0.005 t_{sep}$. Circular points correspond to $t_d = 0.01 t_{sep}$, square points to $t_d = 0.05 t_{sep}$. The dashed line corresponds to the linear dependence given by (A.3). The horizontal dotted lines show $(\Delta q/q_0)_{max}$, see the Appendix.

increasing effective temperature. As would be expected, at $T_{ef} = T$ the geminate pair escape probability does not increase. In this case, the electron photoexcitation results only in the increase of the geminate recombination rate because $D_t/D = nL^2/(6r_c^2\tau_p) \gg 1$ where $\tau_p = t_p D/r_c^2$.

As seen from Fig. 10, the distinction between the enhancement $\Delta q/q_0$, calculated at $\tau_d = t_d/t_{sep} = 0.01–0.05$, and that given by the linear approximation (A.3) is less than 20% at small $nL^2/6r_c^2 < 0.02$, i.e. at $n < 4$. This justifies the employment of the convolution (4.17) at used energies $\Phi_{IR} < 3$ mJ.

References

[1] A. Hummel, Advan. Radiat. Chem. 4 (1974) 1.
[2] M. Pope and C.E. Swenberg, Electronic processes in organic crystals (Clarendon Press, Oxford Univ. Press, Oxford, New York, 1982).
[3] G.R. Freeman, in: Kinetics of nonhomogeneous processes, ed. G.R. Freeman, (Wiley–Interscience, New York, 1987) p. 19.
[4] J.M. Warman, in: The study of fast processes and transient species by electron pulse radiolysis, eds. J.H. Baxendale and F. Busi (Reidel, Dordrecht, 1982) pp. 433–534.
[5] B.S. Yakovlev, Radiat. Phys. Chem. 40 (1992) 37.
[6] B.S. Yakovlev, Radiat. Phys. Chem. 47 (1996) 281.
[7] H.Lu, F.H. Long and K.B. Eisenthal, J. Opt. Soc. Am. 7B (1990) 1511.
[8] Y. Gauduel, S. Pommeret, A. Migus, N. Yamada and A. Antonetti, J. Opt. Soc. Am. 7B (1990) 1528.
[9] M.U. Sander, K. Luther and J. Troe, J. Phys. Chem. 97 (1993) 11489.
[10] C. Pepin, T. Goulet, D. Houde and J.-P. Jay-Gerin, J. Phys. Chem. 98 (1994) 7009.
[11] D. Houde, C. Pepin, T. Goulet and J.-P. Jay-Gerin, Soc. Phot. Opt. Instrum. Eng. 2041 (1993) 139.
[12] M.U. Sander, U. Brummund, K. Luther and J. Troe, J. Phys. Chem. 97 (1993) 8378.
[13] C.L. Braun, S.N. Smirnov, S.S. Brown and T.W. Scott, J. Phys. Chem. 95 (1991) 5529.
[14] B.S. Yakovlev and L.V. Lukin, Advan. Chem. Phys. 60 (1985) 99.
[15] B.S. Yakovlev, K.K. Ametov and G.F. Novikov, Radiat. Phys. Chem. 11 (1978) 77.
[16] L.V. Lukin, A.V. Tolmachev and B.S. Yakovlev, Chem. Phys. Letters 81 (1981) 595.
[17] L.V. Lukin, A.V. Tolmachev and B.S. Yakovlev, High Energy Chem. 16 (1982) 325.
[18] A.V. Tolmachev, L.V. Lukin and B.S. Yakovlev, Soviet J. Chem. Phys. 4 (1987) 908.
[19] L.V. Lukin, A.V. Tolmachev and B.S. Yakovlev, High Energy Chem. 21 (1987) 357.
[20] L.V. Lukin, A.P. Chalov and B.S. Yakovlev, Soviet J. Chem. Phys. 9 (1992) 2578.
[21] L.V. Lukin, A.P. Chalov and B.S. Yakovlev, Soviet J. Chem. Phys. 12 (1994) 1813.
[22] C.L. Braun and T.W. Scott, J. Phys. Chem. 87 (1983) 4776.
[23] T.W. Scott and C.L. Braun, Canad. J. Chem. 63 (1985) 228.
[24] T.W. Scott and C.L. Braun, Chem. Phys. Letters, 127 (1986)501.
[25] C.L. Braun and T.W. Scott, J. Phys. Chem. 91 (1987) 4436.
[26] C.L. Braun and T.W. Scott, Radiat. Phys. Chem. 32 (1988) 315.
[27] L. Onsager, Phys. Rev. 54 (1938) 554.
[28] I.B. Berlman, Handbook of fluorescence spectra of aromatic molecules, 2nd ed. (Academic Press, New York, 1971) p. 168.
[29] S.H. Peterson, M. Yaffe, J.A. Schultz and R.C. Jarnagin, J. Chem. Phys. 63 (1975) 2625.
[30] G.J. Hoffman and A.C. Albrecht, J. Chem. Phys. 94 (1990) 4455.
[31] J.H. Baxendale, C. Bell and P. Wardman, J. Chem. Soc. Faraday Trans. I 69 (1973) 776.
[32] L.V. Lukin, A.V. Tolmachev and B.S. Yakovlev, Bull. Acad. Sci. USSR Chem. Sci. 34 (1985) 2031.
[33] R.M. Marsolais, E.A. Cartier and P. Pfluger, in: Excess electrons in dielectric media, eds. C. Ferradini and J.-P. Jay-Gerin (CRS Press, Boca Raton, 1991) p. 43.
[34] L.V. Lukin, Radiat. Phys. Chem. 40 (1992) 565.
[35] K.H. Schmidt, M.C. Sauer Jr., Y. Lu and A. Liu, J. Phys. Chem. 94 (1990) 244.
[36] Y. Hirata and N. Mataga, J. Phys. Chem. 95 (1991) 1640.
[37] I. Rips and R.J. Silbey, J. Chem. Phys. 94 (1991) 4495.
[38] V.A. Nadtochenko, I.V. Vasil'ev, N.N. Denisov, I.V. Rubtsov, A.S. Lobach, A.P. Moravski and A.F. Shestakov, J. Photochem. Photobiol. A 70 (1993) 153.
[39] L.V. Lukin, A.V. Tolmachev and B.S. Yakovlev, Soviet J. Chem. Phys. 4 (1987) 592.
[40] V.M. Tatevski, Physical and chemical properties of hydrocarbons (Moscow, 1960) p. 374, [in Russian].
[41] T. Shida, S. Iwata and T. Watanabe, J. Phys. Chem. 76 (1972) 3683.
[42] T. Ichikawa and H. Yoshida, J. Chem. Phys. 73 (1980) 1540.
[43] G.F. Novikov and B.S. Yakovlev, Intern. J. Radiat. Phys. Chem. 7 (1975) 479.
[44] S.A. Rice and L. Kevan, J. Phys. Chem. 81 (1977) 847.
[45] S.A. Rice, G. Dolivo and L. Kevan, J. Chem. Phys. 70 (1979) 18.
[46] T. Funabashi, N. Okabe, T. Kimura and K. Fueki, J. Chem. Phys. 75 (1981) 1576.
[47] N. Okabe, T. Kimura and K. Fueki, Can. J. Chem. 61 (1983) 2799.
[48] S.J. Atherton, J.H. Baxendale, F. Busi and A. Kovacs, Radiat. Phys. Chem. 28 (1986) 183.
[49] D.L. Ivanov and B.S. Yakovlev, Khimia Vysokikh Energii 29 (1995) 410, [in Russian].
[50] A. Mozumder and J.L. Magee, J. Chem. Phys. 47 (1967) 939.
[51] H. Sano and A. Mozumder, J. Chem. Phys. 66 (1977) 689.

[52] R. Voltz, in: Excess electrons in dielectric media, eds. C. Ferradini and J.-P. Jay-Gerin (CRS Press, Boca Raton, 1991) pp. 75–104.
[53] J.L. Magee, Can. J. Chem. 55 (1977) 1847.
[54] A.A. Balakin and B.S. Yakovlev, Chem. Phys. Letters 66 (1979) 299.
[55] H.T. Davis, L.D. Schmidt and R.M. Minday, Chem. Phys. Letters 13 (1972) 413.
[56] W.F. Schmidt, Can. J. Chem. 55 (1977) 2197.
[57] W.F. Schmidt, in: Excess electrons in dielectric media, eds. C. Ferradini and J.-P. Jay-Gerin (CRS Press, Boca Raton, 1991) p. 127.
[58] R.A. Holroyd and R.L. Russel, J. Phys. Chem. 78 (1974) 2128.
[59] J. Bullot and M. Gauthier, Can. J. Chem. 55 (1977) 1821.
[60] B. Raz and J. Jortner, Chem. Phys. Letters 4 (1969) 155.
[61] R.A. Holroyd, J.M. Preses and N. Zevos, J. Chem. Phys. 79 (1983) 483.
[62] R.A. Holroyd, S. Tames and A. Kennedy, J. Phys. Chem. 79 (1975) 2857.
[63] F.F. Brazgun, L.V. Lukin, V.A. Nadtochenko and I.V. Rubtsov, J. Chim. Phys. (1996) accepted.
[64] H.T. Choi, D.S. Sethi and C.L. Braun, J. Chem. Phys. 77 (1982) 6027.
[65] E.W. Schlag and R.D. Levine, J. Phys. Chem. 96 (1992) 10608.
[66] R. Katoh and M. Kotani, Chem. Phys. Letters 188 (1992) 80.
[67] A.A. Balakin, L.V. Lukin, A.V. Tolmachev and B.S.Yakovlev, High Energy Chem. 15 (1981) 96.
[68] M. Tachiya and A. Mozumder, J. Chem. Phys. 62 (1975) 2125.